

Magnetron Sputtered Silicon Coatings as Oxidation Protection for Mo-Based Alloys

Ronja Anton,* Nadine Laska, Uwe Schulz, Susanne Obert, and Martin Heilmaier

Mo-based alloys with solidus temperatures around and above 2000 °C are attractive high-temperature structural materials for future applications in the hot section of gas turbines. However, their oxidation behavior is poor due to pesting starting at 600 °C and nonprotective oxide growth at temperatures above 1000 °C. To ensure a sufficient oxidation resistance over a wide temperature range, protective coatings become inevitable. Herein, silicon coatings have been applied by magnetron sputtering on Mo-9Si-8B and on titan–zirconium–molybdenum alloy (TZM). The coating architecture is designed to minimize the intercolumnar gaps and porosity, thereby increasing the density. Specimens are tested at 800 and 1200 °C in air isothermally for up to 300 h. The focus is put on the chemical reactions at the coating–substrate interface, the phase formation, and the evolution of the thermally grown oxide. An initially globular SiO₂ evolves into a uniform SiO₂ layer providing excellent oxidation protection. The investigations reveal a rather slow interdiffusion between the coating and the alloys when tested in air. At the coating–substrate interface exclusively, the Mo₃Si phase develops. Finally, the phase formation at the coating–substrate interface is studied in detail for various heat treatments in air and vacuum.

further increase in operating temperature with this material is unlikely due to the limit given by the solidus temperature of Ni-based superalloys.^[2,3] Mo-based alloys with solidus temperatures around and above 2000 °C are attractive high-temperature structural materials to overcome those limits. Therefore, these alloys are potential candidates for future applications in the hot section of gas turbines. Alloys with a composition in the three-phase field—Mo_{ss}, Mo₃Si, and Mo₅SiB₂—show favorable mechanical properties.^[2–4] Mo_{ss} forms a continuous matrix that provides sufficient fracture toughness, whereas the intermetallic phases Mo₃Si and Mo₅SiB₂ ensure promising creep resistance. Their low-tensile ductility at room temperature and oxidation behavior are still challenging. The oxidation and the creep behavior of these alloys can be somewhat improved by alloying with titanium,^[5–8] which is also the topic of a companion paper in the same issue (see Matthias Weber et al., Effect of Water


1. Introduction

The efficiency of a gas turbine can be improved by increasing the gas inlet temperature.^[1–3] Nowadays, aeroengines are limited by the temperature capability of the materials used in the first stages of the high-pressure turbine. Ni-based superalloy blades are provided with internal cooling and coatings consisting of an outer thermal barrier layer and a bond coat to connect it to the respective substrate. Although they show excellent performance, a

Vapor on the Oxidation Behavior of the Eutectic High-Temperature Alloy Mo-20Si-52.8Ti, this issue). However, the general oxidation behavior of Mo-based alloys is poor due to evaporation of MoO₃ at temperatures below 1000 °C, well known as the pesting regime,^[9] and rapid oxide growth at temperatures above 1000 °C. To ensure a sufficient oxidation resistance over a wide temperature range, protective coatings become inevitable. A thermochemical compatible interface between coating and alloy as well as a coefficient of thermal expansion (CTE) which is close to that of the Mo-based alloys are prerequisites for a good coating performance. Substantial improvements could be demonstrated by Mo, Si, and B containing coatings applied by chemical vapor deposition (CVD) or physical vapor deposition (PVD) techniques. The CVD coatings were produced by copack cementation of Si, Si, and B, or Si and Al. After heat treatments and testing, the coatings mostly show either an oxidation protection based on silicon dioxide, borosilicate, or Al₂O₃.^[10–13] The magnetron sputtered PVD coatings with a thickness of around 5–10 μm developed in our previous work showed promising oxidation behavior. Three-phase coatings consisting of Mo₅Si₃, MoSi₂, and MoB as well as single-phase MoSi₂ and MoB coatings have been investigated. Mo₅SiB₂ (T2) was introduced as diffusion barrier due to its high atomic packing density and to avoid early coating degradation by interdiffusion with the alloy.^[2,14] In addition, aluminum containing coatings based on Mo–70Al and Mo–47Si–24Al have been investigated

R. Anton, Dr. N. Laska, Prof. U. Schulz
German Aerospace Center (DLR)
Institute of Materials Research
Linder Hoehe, 51147 Cologne, Germany
E-mail: ronja.anton@dlr.de

S. Obert, Prof. M. Heilmaier
Institute for Applied Materials (IAM-WK)
Karlsruhe Institute of Technology (KIT)
Engelbert-Arnold-Straße 4, 76131 Karlsruhe, Germany

 The ORCID identification number(s) for the author(s) of this article can be found under <https://doi.org/10.1002/adem.202000218>.

© 2020 The Authors. Published by WILEY-VCH Verlag GmbH & Co. KGaA, Weinheim. This is an open access article under the terms of the Creative Commons Attribution License, which permits use, distribution and reproduction in any medium, provided the original work is properly cited.

DOI: 10.1002/adem.202000218

as well including the application of thermal barrier coatings on top.^[15]

In this research, a different approach has been chosen. To establish a larger coating thickness by magnetron sputtering, boron was avoided in the procedure because it possesses a poor sputter rate. Furthermore, a one layer concept was pursued for simplification. Silicon is widely accepted as oxidation protection layer and used by various researchers for SiC/SiC ceramic matrix composites as a bond coat in environmental barrier coating systems.^[16,17] Therefore, Si has been used as a PVD coating to protect Mo-based alloys. Its oxide SiO₂ can emerge in various polymorphs—in most studies cristobalite is found. This so-called thermally grown oxide (TGO) is one of the slowest forming oxides known to date being able to withstand several thousand hours of oxidation at temperatures above 1100 °C. Moreover, silicon shows favorable mechanical properties because it becomes ductile at temperatures above 600 °C.^[18,19] The main emphasis of this study is to develop and characterize a single layer coating based on silicon for the Mo-9Si-8B alloy to ensure oxidation protection up to 1200 °C.

2. Experimental Section

The Mo-based alloy (Mo-9Si-8B in at%) was fabricated at Karlsruhe Institute of Technology (KIT) by arc melting the high-purity elements Mo, Si, and B with respective purities of 99.99%, 99.8%, and 99%. An arc-melter of type AM/0.5 by Edmund Buehler GmbH was used and the arc-melting procedure was performed in a water-cooled copper crucible under Ar atmosphere, as described in detail by Obert et al.^[20] During arc melting of various Mo–Si–X alloys, the contamination by oxygen was routinely measured by hot gas carrier extraction. Typically, between 150 and 350 wt ppm of oxygen were detected which is substantially lower as the values observed in PM-processed material being above 2000 wt ppm of oxygen.^[21] A homogenous elemental distribution was ensured by repeating the melting procedure multiple times and the final chemical composition was measured and confirmed to vary less than 0.5 wt% from the target chemical composition. As expected from the phase diagram, the produced Mo-9Si-8B alloy consisted of the phases Mo₅Si (bcc), Mo₃Si (A15), and Mo₅SiB₂ (T2).^[22] For the coating trials, the alloy was used in the as-cast state with substrate dimensions of 10 × 15 × 2 mm. For comparison, a commercial titan–zirconium–molybdenum alloy (TZM) with the nominal composition of Mo-0.5 Ti-0.08 Zr-0.01–0.04 C (in at%) provided by Plansee AG, Reutte, Austria, has been used as well.

The Si coating was applied using a batch-type magnetron sputtering facility (Z400, Systec SVS vacuum coatings, Karlstadt, Germany). Before coating deposition, specimens were cleaned by Ar⁺-ion etching to activate the specimen surface. Two dense polycrystalline disks of Si with a diameter of 100 mm were utilized as targets that were placed in a face-to-face arrangement. DC sputtering was performed at 1 kW target power to achieve a total thickness of the coating between 25 and 50 μm. After first successful tests with a 50 μm-thick Si coating, the thickness has been halved because the interdiffusion between coating and Mo–Si substrates was slower than expected. The majority of the experiments had been carried out on the thinner coatings.

The total pressure during deposition was 0.45 Pa in Ar atmosphere (flow rate at 25 sccm). During the deposition process, the substrate temperature reached about 100 °C without additional heating. The deposition rate was around 6 μm h⁻¹. Samples were constantly rotated during the application of the coating ensuring a full coverage of the samples by the coating and a nearly all-around constant thickness. Due to variation in sample position with respect to the sputtering source, a slight variation in coating thickness was noticeable.

As the Si coating was X-ray amorphous after the deposition process, a crystallization treatment was applied for 1 h at 900 °C in air. To achieve a nearly dense coating and to rapidly close the intercolumnar gaps, the specimen underwent a rapid heating up during crystallization as well as during the initial oxidation. This temperature was chosen to guarantee the crystallization of Si which was confirmed by high-temperature X-ray diffraction (XRD) investigations, and to compare the present results to previous data obtained on similar coatings applied on SiC substrates. Afterward, the coated specimens underwent isothermal oxidation testing up to 300 h in lab air in a box furnace. Two temperatures had been used for testing, 800 and 1200 °C, to investigate both peeling and high temperature oxidation behavior. The crystallization treatment and isothermal oxidation had been performed without a cooling period in between. To compare the phase formation at the interface between coating and alloy in vacuum (10⁻⁵ mbar) and in lab air, a comparison study had been done with silicon-coated TZM.

For all coatings, phase analyses were performed using XRD (Bruker D8 Advance, Cu Kα radiation, EVA/Topas 4.2 software package, Bruker AXS, Karlsruhe, Germany). Microstructural analyses were carried out by scanning electron microscopy (SEM) (DSM Ultra 55, Carl Zeiss NTS, Wetzlar, Germany) equipped with an energy-dispersive X-ray spectroscopy (EDS) system (Aztec, Oxford Instruments, Abingdon, UK). EDS analyses have been performed at 15 kV. For further analysis, two lamellae were produced by a focused ion beam (FIB) (Dual Beam FEI Helios, FEI Philips, The Netherlands). To analyze the interdiffusion zone (IDZ), transmission electron microscopy (TEM) had been carried out using imaging, EDS analyses, and electron diffraction measurements applying selected area diffraction (SAD) (Tecnai F30 TEM/STEM FEI Philips, The Netherlands).

3. Results

3.1. Isothermal Oxidation Behavior of the Si-Coated Mo-Based Alloys

The as-coated silicon coating possesses excellent adhesion on both substrate alloys. It has a columnar structure evident in cross section and a cauliflower pattern in top view (see **Figure 1a,d** for the TZM alloy substrate). This specimen serves as a reference micrograph to compare the tested coating to the initial as-coated state after the deposition. XRD, not shown here, proofed that the coatings were amorphous in this state. After the initial heat treatment for 1 h at 900 °C in lab air, the Si coatings crystallized.

In **Figure 1b**, the coating is shown after 1 h of crystallization annealing at 900 °C and 10 h of isothermal testing at 1200 °C in air. The SEM cross section in **Figure 1b** shows that

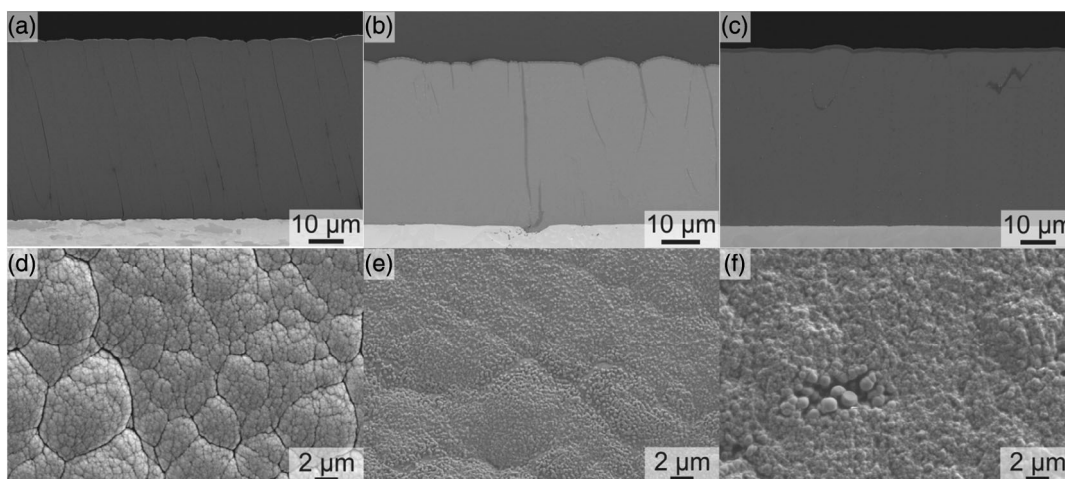


Figure 1. Silicon coating on Mo-based alloys: a–c) cross sections and d–f) top views. a,d) TZM substrate in the as-coated state; b,e) Mo-9Si-8B substrate isothermally tested for 10 h at 1200 °C; c,f) Mo-9Si-8B substrate isothermally tested for 100 h at 1200 °C.

intercolumnar gaps get closed already after 10 h of exposure due to the oxidation of silicon. A dense SiO_2 TGO is visible on top of the surface of the coating which shows also a bubbly structure (see Figure 1e). After 100 h heat treatment, the only change in the coating system is the obvious growth of the SiO_2 TGO that increased in thickness up to 1.1 μm (Figure 1c). The top view shows smaller bubbles of SiO_2 that appear now fully dense (see Figure 1f).

In Figure 1b,c, the formation and growth of a thermally grown oxide are evident after 10 and 100 h testing at 1200 °C on Mo-9Si-8B. By analyzing the thicknesses of the TGO with increasing time which is exemplified in Figure 2 until 10 h (Figure 2a), until 100 h (Figure 2b), and until 300 h (Figure 2c), a parabolic growth rate of the thermally grown SiO_2 can be confirmed (see Figure 3). The SiO_2 consists of the cristobalite phase which has been proven by XRD. The TGO was dense and the initially formed bubbles seemed to be connected to the dense layer forming afterward. The bubbles were not included in the determination of the TGO thickness.

To investigate the potential influence of boron on the formation of the SiO_2 bubbles, oxidation of the silicon coating has also been investigated using a TZM substrate which contains no boron. Figure 4a shows that after a crystallization treatment at 900 °C for 1 h and 30 min at 1200 °C, both done in air, no bubble-shaped structures were visible on the surface. After a total oxidation time of 2 h at 1200 °C, the surface is covered by bubbles that appear similar to the morphology formed on Mo-9Si-8B

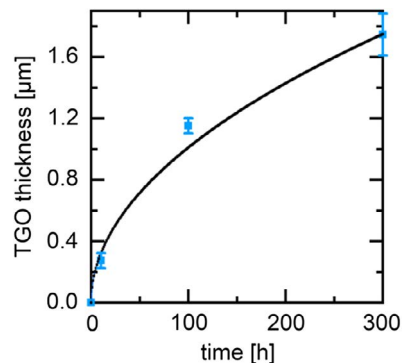


Figure 3. Growth rate of the thermally grown SiO_2 layer versus exposure time at 1200 °C in lab air.

(see Figure 4b). Again, the bubbles are well connected to the dense silica layer that forms underneath during prolonged oxidation of 5 h (see Figure 4c).

The TEM-EDS mapping in Figure 5 shows an FIB lamella of the 10 h tested silicon coating on a Mo-9Si-8B substrate. The silicon coating is clearly visible as well as the SiO_2 TGO. A weak molybdenum signal is detectable in some isolated areas. There is no clear accumulation of Mo within the bubbles, although some Mo signals appear locally in the gaps between the silica bubbles.

To additionally investigate the potential impact of MoO_3 sublimation that starts at about 700 °C on the coating behavior,

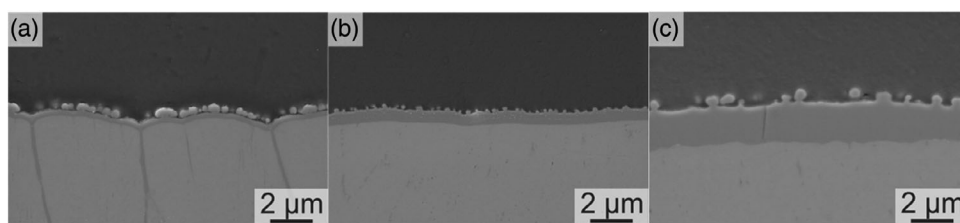


Figure 2. Formation of the thermally grown oxide consisting of SiO_2 with SiO_2 bubbles on a Si-coating on a Mo-9Si-8B substrate during isothermal testing for a) 10 h, b) 100 h, and c) 300 h at 1200 °C in lab air.

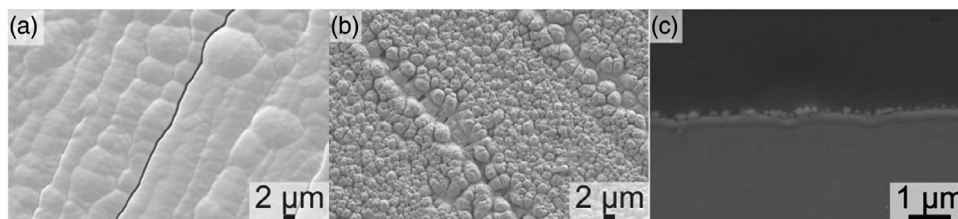


Figure 4. SEM pictures of the silicon coating surface on TZM substrates tested for a) 1 h at 900 °C and 30 min at 1200 °C in air; b) 1 h at 900 °C and 2 h at 1200 °C in air showing a bubbly SiO₂ structure; and c) 1 h at 900 °C and 5 h at 1200 °C in air showing the bubbly structure in the cross section.

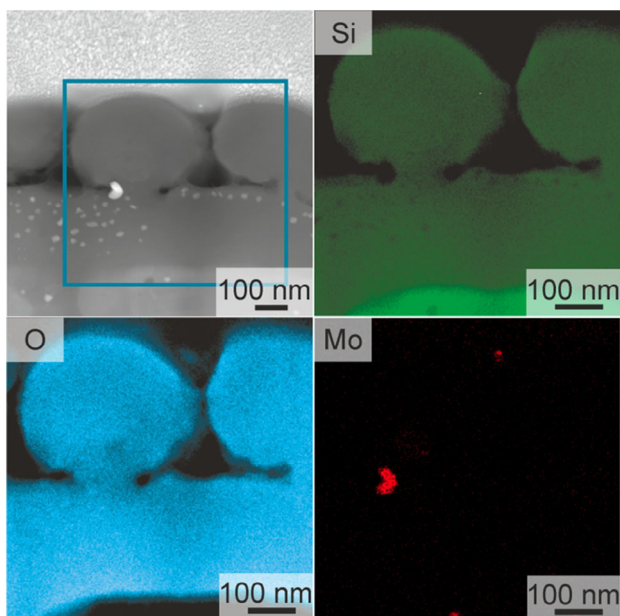


Figure 5. TEM-EDS mapping of the TGO done on a FIB lamella of the 10 h isothermal tested silicon coating on a Mo-9Si-8B substrate at 1200 °C.

an isothermal heat treatment has been applied at 800 °C for 100 h after the crystallization treatment for 1 h at 900 °C. The result shown in **Figure 6** reveals a relatively dense coating on a Mo-9Si-8B substrate without a visible TGO. A few columns do not seem to be sealed by SiO₂, but do not lead to oxidation of the substrate. The top view shows a quite dense coating replicating the substrate roughness and showing remaining signs of the

typical PVD columnar structure, but to a much lower degree compared with the as-coated condition shown in **Figure 1a,d**. SEM-EDS (not shown here) proved that no Mo is detected in the coating.

3.2. Reaction between Coating and Substrate during Isothermal Oxidation

During oxidation, an IDZ can be observed that slowly grows with time. **Figure 7** shows the increase in thickness of this zone after 10 h (**Figure 7a**), 100 h (**Figure 7b**), and 300 h (**Figure 7c**) at 1200 °C testing temperature. The growth rate of the IDZ versus the exposure time is shown in **Figure 8** where it follows a parabolic growth rate. Although some pores appear at the interface between substrate and coating after 300 h, mainly located within the silicon in contact to the IDZ, the adhesion of the coating is still strong which assures the oxidation protective potential of the Si coating for the Mo-9Si-8B alloy.

To clarify which phases have formed at the interface and in the IDZ, a sample tested for 300 h was analyzed in the TEM in different locations (see **Figure 9**). **Figure 9a** shows a high-angle annular dark-field image (HAADF) of the FIB lamella with the region of interest. The analysis clearly proves that the interdiffusion zone consists exclusively of the Mo₃Si phase. Therefore, two grains have been shown in **Figure 9b,c**. Comparing two different lamellae yielded that the IDZ is rather inhomogeneous in thickness. In **Figure 9**, the IDZ thickness is identical to the Mo₃Si grain size because it consists only of one grain in thickness, whereas in other parts several Mo₃Si grains are forming above each other further into the substrate, thereby resulting in a thicker IDZ.

Most of the investigations in the literature about the interdiffusion of silicon and molybdenum are done with the pure

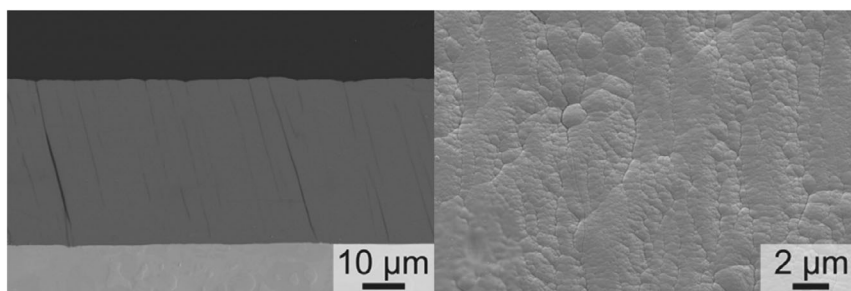


Figure 6. Silicon-coated Mo-9Si-8B substrate isothermally tested for 100 h at 800 °C (cross section left and top view right).

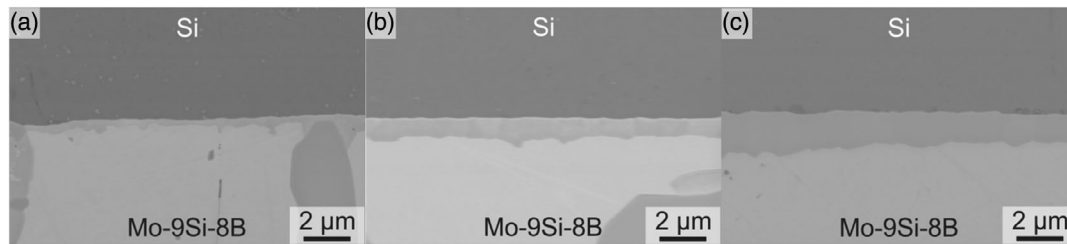


Figure 7. Interdiffusion zone of a silicon coating on a Mo-9Si-8B substrate isothermally tested for a) 10 h, b) 100 h, and c) 300 h at 1200 °C.

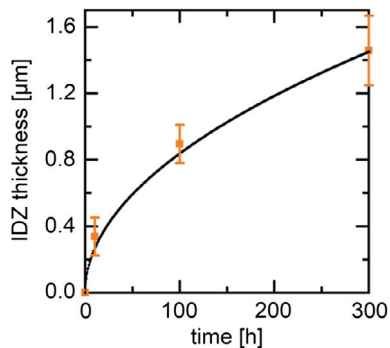


Figure 8. Growth rate of the interdiffusion zone between silicon coating and Mo-9Si-8B substrate versus exposure time at 1200 °C in lab air.

elements under vacuum.^[23] To separate the phases within the IDZ clearly from the phases in the substrate and for a better comparison with the literature, further investigations have been done on TZM coated with silicon. To study the influence of the annealing atmosphere on the interdiffusion behavior, a vacuum heat treatment was compared with a lab air heat treatment, applying the same time and temperature.

After vacuum annealing for 1 h at 900 °C and 5 h at 1200 °C, the phases Mo_5Si_3 and MoSi_2 evolved to form the IDZ (see **Figure 10a**). Furthermore, most of the original Si coating spalled off this IDZ leaving it exposed to the atmosphere. In the EDS line scans using SEM (**Figure 10**), substrate, IDZ, and coating were analyzed. The sample annealed in air shows the same IDZ already shown in **Figure 7**. There, the line scan (**Figure 10b**) illustrates the formation of Mo_3Si in the IDZ.

Furthermore, it reveals an oxygen content of about 38 at% (measured by EDS) in the IDZ of the specimen tested in air, whereas there was no oxygen found in the IDZ of the vacuum annealed sample (**Figure 10a**). **Figure 11** shows results of the XRD investigation. As the Si coatings used for this investigation were intentionally only 25 μm thick, the XRD information extracted from those samples also provide results on the phases within the IDZ located underneath the Si. Thus, diffraction peaks of the Mo_3Si phase are also present for the air-tested sample, whereas the Mo_5Si_3 phase is detectable for the vacuum-tested sample. Due to the small peak heights of those phases, **Figure 11** is shown with a logarithmic scale.

Obviously, different phases developed within the IDZ after the vacuum (MoSi_2 , Mo_5Si_3) and the lab air (MoSi_3) treatment as confirmed by EDS and XRD. The development of Mo_5Si_3 and MoSi_2 in the IDZ is conclusive for the vacuum annealed specimen. For the lab air treated specimen, the interdiffusion phase shows exclusively the composition of Mo_3Si and some excess oxygen.

4. Discussion

4.1. Oxidation of Silicon on Molybdenum-Based Alloys

The applicability of silicon as an oxidation protective coating on a Mo-9Si-8B alloy was successfully demonstrated up to 300 h at 1200 °C. **Figure 2** and **3** show the exclusively diffusion controlled parabolic growth rate of the thermally grown SiO_2 layer on silicon which has already been studied in detail for other substrate materials.^[24] XRD scans confirm that the TGO forming here is cristobalite which is in accordance with most findings on silica

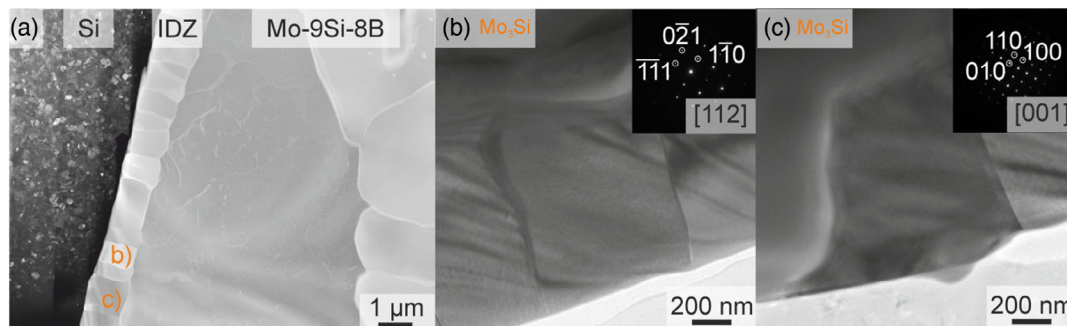


Figure 9. TEM picture of the silicon coated Mo-9Si-8B lamella isothermally tested for 300 h at 1200 °C; a) HAADF overview of lamella with interdiffusion zone; b) grain b within interdiffusion zone and diffraction pattern; and c) grain c within interdiffusion zone and diffraction pattern with viewing directions.

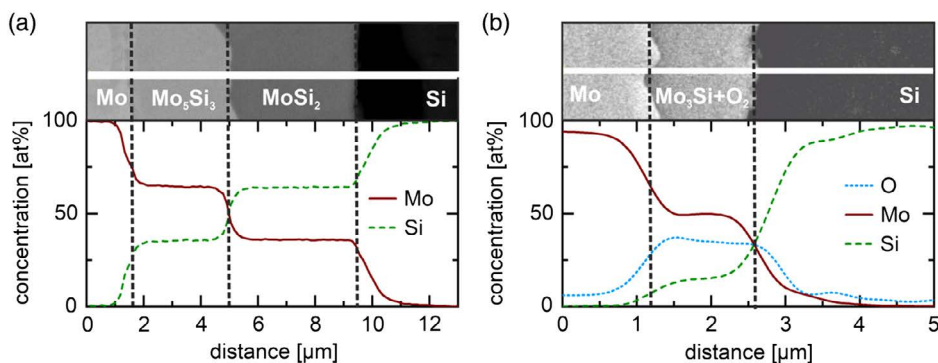


Figure 10. SEM-EDS line scans of the silicon coated TZM substrate tested for 1 h at 900 °C and 5 h at 1200 °C: a) in vacuum; b) in air.

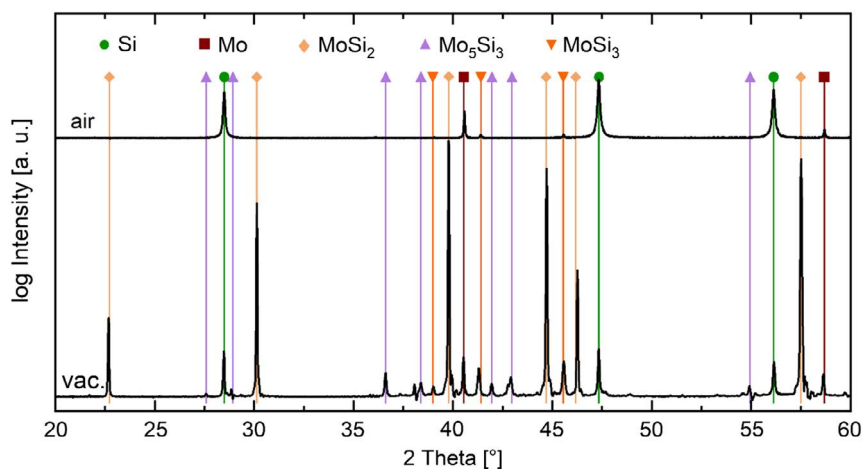


Figure 11. XRD scan of the silicon coated TZM substrate tested for 1 h at 900 °C and 5 h at 1200 °C in air and vacuum.

formation on SiC and pure Si, although the temperatures for cristobalite formation given in the phase diagram under equilibrium conditions are higher.^[24,25] In our previous work on HfO₂-doped and pure silicon coatings on SiC substrates, we could confirm that a TGO consisting of cristobalite at about the same testing temperatures of 1250 °C forms.^[24] This is consistent with findings of ref. [26] where potential reasons for favored cristobalite formation at lower temperatures are discussed in detail.

The TGO growth rate found in the present work is in the same order as the one for PVD silicon coatings on SiC substrates, although the oxidation temperature was 50 °C higher there.^[24] This implies that the Mo-based substrate does not influence the oxidation kinetics of this coating much. The SiO₂ polymorph cristobalite undergoes a high/low-temperature phase transitions with a CTE difference of about $7.2 \times 10^{-6} \text{ K}^{-1}$ and a volume change of approximately 2.8%. This transition causes potentially tension between the SiO₂ layer and the nonoxidized Si coating.^[24,25,27] However, as there was no severe oxide spallation or cracking of the TGO detected after the 300 h testing applied here, the coating provides great potential for prolonged oxidation protection of Mo-based alloys. Interestingly, the growth of the silica starts by forming bubbles on top of the surface. After an incubation period of 30 min where no bubbles form at 1200 °C, they are already present after 120 min of oxidation

(see Figure 4). A dense and continuous TGO layer evolves as well, most likely in parallel to the formation of bubbles. Silica bubbles were not observed for the same PVD silicon coating applied on SiC substrates.^[24] The bubbles do not seem to grow or increase in number, but stay nearly constant and unchanged over the entire annealing time up to 300 h. The silica grows continuously underneath the bubbles which do not change the local oxidation behavior substantially. This leads to the conclusion that some sort of gaseous species might form during the initial SiO₂ formation which initiate the bubble formation. As the bubbly structure appears on a TZM substrate as well as on the Mo-9Si-8B alloy, boron can most likely be excluded and molybdenum or the volatile MoO₃ is suspected to be trapped in these bubbles. MoO₃ forms and volatilizes already at temperatures around 650 °C.^[8] After the growth of both the dense TGO and the inter-diffusion zone, no MoO₃ seems to be able to move to the surface. Therefore, it is likely that small amounts of MoO₃ diffuse through the silicon coating onto the surface. The formation of a dense and continuous TGO layer is already completed after 5 h at 1200 °C. The TEM-EDS in Figure 5 provides at least some hints pointing toward molybdenum causing the initial formation of the silica bubbles. Figure 6 shows that the amount of MoO₃ reaching the surface seems to be quite small because no internal substrate oxidation can be found after 100 h at 800 °C. To the best knowledge of the authors, the effect of an initially bubbly silica

formation on a silicon coating has not been published so far. More detailed research has to be conducted in the near future to give more insight into the formation mechanism of the bubbles.

In the initial stages of oxidation, the columnar structure of the silicon coating gets dense by rapid formation of silica along the intercolumnar gaps. This densification seals the gaps and prevents further inward diffusion of oxygen because all gaps are filled by silica which possesses a rather low oxygen diffusivity. It is possible that those early stages of oxygen inward diffusion, silica formation in the intercolumnar gaps, transient formation of (volatile) Mo-oxides, and formation of silica bubbles are interconnected which is the topic of ongoing studies. However, as the Si coating can protect the Mo-9Si-8B substrate successfully from pest-oxidation after 100 h at 800 °C, the process of Mo-oxide volatilization might even start at more elevated temperatures drastically.

4.2. Interdiffusion of Silicon and Molybdenum in Different Atmospheres

The interdiffusion of silicon and molybdenum is widely investigated and understood in atmospheres that do not contain oxygen. In this case, silicon diffuses much faster into molybdenum than vice versa to form the phases MoSi₂, Mo₅Si₃, and lastly Mo₃Si. MoSi₂ is thereby the most dominant phase followed by Mo₅Si₃. Mo₃Si occurs later as a thin layer directly on the molybdenum.^[12,28–31] In the present investigation, silicon-coated TZM follows the same pattern when heat treated under vacuum (see Figure 10 and 11). The phase diagram of Mo–Si confirms that all three phases are possible to evolve at temperatures around 1200 °C. The study of Yoon et al. provides evidence that silicon is not able to adhere over longer annealing times to the Mo–silicide phases due to the large mismatch of the CTE (Si: $3.8 \times 10^{-6} \text{ K}^{-1}$, MoSi₂: $9.5 \times 10^{-6} \text{ K}^{-1}$).^[32,33] In contrast to the scenario under vacuum described earlier, under oxygen containing atmosphere such as lab air the silicon coating on the TZM substrate behaves differently in the current study. In this case only the Mo₃Si phase forms predominantly by growing into the TZM substrate (see in Figure 10 and 11). The CTE of Mo₃Si is about $6.03 \times 10^{-6} \text{ K}^{-1}$ ^[34] which fits better to both the CTE of Mo-based alloys, silicon and silica.

Oxygen has been detected in the EDS line scan in substantial amounts in this phase. As there is no evidence of a second phase forming other than MoSi₃, the oxygen seems to be dissolved in this phase. The study also shows that the IDZ of MoSi₃ increases in thickness with time (Figure 8) in air. Yoon et al. describe that the Mo₃Si phase grows into the Mo substrate rather than forming in the contact zone between Si and Mo. The same has been found here, i.e., formation of Mo₃Si by mostly inward diffusion of silicon and formation of the phase within the former Mo alloy (see Figure 7). Silicon is in this case the faster diffusing species as seen before in the vacuum annealing, too.^[35] This is in good agreement with the literature data, clearly indicating that silicon is the more mobile element in all relevant Mo–Si phases due to the much higher defect concentration within the Si sublattices.^[23] A few studies aimed already at explaining the influence of oxygen on the interdiffusion between those two elements.^[28,32] Although none of the studies found the total suppression of

MoSi₂ and Mo₅Si₃ as demonstrated here, the explanation given there seems to hold for the present case as well. Yoon et al. concluded that the MoSi₂ growth rate and activation energy are heavily influenced by impurities like oxygen.^[32] The growth rate decreases in an oxygen containing atmosphere which is in good agreement with the results found in this study. The present findings clearly show that no other phase than Mo₃Si forms in oxygen containing atmosphere. Moreover, it dissolves substantial amounts of oxygen because there is no known phase being constituted by all the three elements: Mo, Si, and O. It could be possible that oxygen supports the formation of the Mo₃Si phase rather than the Si-rich Mo silicides. How oxygen hinders the silicon to diffuse further into molybdenum and thereby impeding the development of silicon-rich Mo silicide could not be finally clarified within this study. But this phenomenon can also be found in Rastogi et al.^[28] There SiO₂ formed at the silicon/molybdenum interface hinders the formation of silicides. In this study, no SiO₂ could be found below the Si coating until now, which confirms the excellent oxidation protection of this PVD layer for Mo-based alloys.

5. Conclusion

In this study, a simple coating with pure Si has been successfully applied as single layer for oxidation protection by magnetron sputtering on Mo-based alloys for the first time. The coating was able to protect the Mo-9Si-8B alloy until 300 h of isothermal exposure at 1200 °C in lab air due to the development of a dense thermally grown silica scale on top. The protective Si coating showed excellent adhesion on the Mo-9Si-8B substrate during prolonged oxidation. In the initial phase of oxidation, the SiO₂ formed a bubbly structure. The silica bubbles did not change with time, whereas the dense and slowly growing TGO formed underneath and thickened with time. At intermediate temperatures of 800 °C, the pest-oxidation could be successfully suppressed by the Si coating up to 100 h.

An interdiffusion zone consisting exclusively of the Mo₃Si phase has been formed during annealing in air by silicon inward diffusion into the Mo-based alloy. This phase contains substantial amounts of oxygen. During 300 h testing at 1200 °C, this slow growing interdiffusion zone possess a varying thickness in the order of 1–2 μm. Testing in vacuum showed the formation of an interdiffusion zone being about 8 μm thick and containing the MoSi₂ and the Mo₅Si₃ phases where no oxygen has been detected. It seems to be reasonable that oxygen containing atmospheres favor the formation of Mo₃Si while suppressing the MoSi₂ and Mo₅Si₃ phases.

Acknowledgements

This work was conducted under the financial support of Deutsche Forschungsgemeinschaft (DFG) within the framework of grants no. Schu1372/7-1 and HE 1872/33-1 which is gratefully acknowledged. For the scientific and technical support at the German Aerospace Centre, the authors thank V. Leisner, P. Bauer, A. Handwerk, P. Herzog, and F. Kreps.

Conflict of Interest

The authors declare no conflict of interest.

Keywords

interdiffusion processes, magnetron sputtering, oxidation behavior, Si-based coatings, thermally grown silica

Received: February 21, 2020

Revised: April 3, 2020

Published online:

-
- [1] J. H. Perepezko, *Science* **2009**, 326, 1068.
 [2] A. Lange, R. Braun, *Corros. Sci.* **2014**, 84, 74.
 [3] M. R. Middlemas, J. K. Cochran, *JOM* **2010**, 62, 20.
 [4] J. H. Perepezko, *Int. J. Refract. Metal. Hard Mater.* **2018**, 71, 246.
 [5] M. A. Azim, B. Gorr, H. J. Christ, O. Lenchuk, K. Albe, D. Schliephake, M. Heilmaier, *Intermetallics* **2017**, 90, 103.
 [6] D. Schliephake, A. Kauffmann, X. Cong, C. Gombola, M. Azim, B. Gorr, H.-J. Christ, M. Heilmaier, *Intermetallics* **2019**, 104, 133.
 [7] S. Burk, B. Gorr, H.-J. Christ, D. Schliephake, M. Heilmaier, C. Hochmuth, U. Glatzel, *Scr. Mater.* **2012**, 66, 223.
 [8] D. Schliephake, C. Gombola, A. Kauffmann, M. Heilmaier, J. H. Perepezko, *Oxidat. Metals* **2017**, 88, 267.
 [9] M. A. Azim, D. Schliephake, C. Hochmuth, B. Gorr, H.-J. Christ, U. Glatzel, M. Heilmaier, *JOM* **2015**, 67, 2621.
 [10] J. H. Perepezko, T. A. Sossaman, M. Taylor, *J. Thermal Spray Technol.* **2017**, 26, 929.
 [11] S. Majumdar, *Appl. Surface Sci.* **2017**, 414, 18.
 [12] S. Majumdar, I. Sharma, I. Samajdar, P. Bhargava, *J. Electrochem. Soc.* **2008**, 155, D734.
 [13] K. Choi, W. Yang, K.-H. Baik, Y. Kim, S. Lee, J. S. Park, *Oxidat. Metals* **2019**, 92, 423.
 [14] A. Lange, R. Braun, M. Heilmaier, *Intermetallics* **2014**, 48, 19.
 [15] A. Lange, R. Braun, U. Schulz, *Mater. High Temp.* **2017**, 35, 195.
 [16] K. N. Lee, in *Ceramic Matrix Composites: Materials, Modeling and Technology* (Eds: N. P. Bansal, J. Lamon), John Wiley & Sons, Hoboken, NJ **2015**, pp. 430–451.
 [17] B. T. Richards, H. N. G. Wadley, *J. Eur. Ceram. Soc.* **2014**, 34, 3069.
 [18] W. D. Sylwestrowicz, *Philos. Mag.* **1962**, 7, 1825.
 [19] D. Zhu (NASA EBC and CMC System Development), *NASA GRC-E-DAA-TN14696* **2014**.
 [20] S. Obert, A. Kauffmann, M. Heilmaier, *Acta Mater.* **2020**, 184, 132.
 [21] M. Krüger, S. Franz, H. Saage, M. Heilmaier, J. H. Schneibel, P. Jehanno, M. Böning, H. Kestler, *Intermetallics* **2008**, 16, 933.
 [22] R. Sakidja, J. Park, J. Hamann, J. Perepezko, *Scr. Mater.* **2005**, 53 723.
 [23] S. Prasad, A. Paul, *Intermetallics* **2011**, 19, 1191.
 [24] R. Anton, V. Leisner, P. Watermeyer, M. Engstler, U. Schulz, *Acta Mater.* **2020**, 183, 471.
 [25] B. T. Richards, S. Sehr, F. de Franqueville, M. R. Begley, H. N. G. Wadley, *Acta Mater.* **2016**, 103, 448.
 [26] E. J. Opila, *J. Am. Ceram. Soc.* **1994**, 77, 730.
 [27] H. Salmang, H. Scholze, R. Telle, *Keramik*, Springer, Berlin, Germany **1982**.
 [28] R. S. Rastogi, V. D. Vankar, K. L. Chopra, *Thin Solid Films* **1992**, 213, 45.
 [29] J.-K. Yoon, J.-Y. Byun, G.-H. Kim, J.-S. Kim, C.-S. Choi, *Thin Solid Films* **2002**, 405, 170.
 [30] M. Salamon, A. Strohm, T. Voss, P. Laitinen, I. Riihimäki, S. Divinski, W. Frank, J. Räisänen H. Mehrer, *Philos. Mag.* **2006**, 84, 737.
 [31] J.-Y. Byun, J.-K. Yoon, G.-H. Kim, J.-S. Kim, C.-S. Choi, *Scr. Mater.* **2002**, 46, 537.
 [32] J. K. Yoon, J. Y. Byun, G. H. Kim, J. S. Kim, C. S. Choi, *Surf. Coat. Tech.* **2002**, 155, 85.
 [33] M. Rice, K. Sarma, *J. Electrochem. Soc.* **1981**, 128, 1368.
 [34] J. H. Schneibel, C. T. Liu, D. S. Easton, C. A. Carmichael, *Mater. Sci. Eng. A* **1999**, 261, 78.
 [35] J. K. Yoon, J. K. Lee, K. H. Lee, J. Y. Byun, G. H. Kim, K. T. Hong, *Intermetallics* **2003**, 11, 687.